

# Estimation of the vascular fraction in brain tumors by VERDICT correlated with Perfusion MRI

Matteo Figini<sup>1</sup>, Antonella Castellano<sup>2</sup>, Valentina Pieri<sup>2</sup>, Samira Bouyagoub<sup>3</sup>, Andrea Falini<sup>2</sup>, Daniel C Alexander<sup>1</sup>, Mara Cercignani<sup>3</sup>, and Eleftheria Panagiotaki<sup>1</sup>

<sup>1</sup>Centre for Medical Image Computing, Department of Computer Science, University College London, London, United Kingdom, <sup>2</sup>Neuroradiology Unit and CERMAC, Vita-Salute San Raffaele University and IRCCS San Raffaele Scientific Institute, Milano, Italy, <sup>3</sup>Clinical Imaging Sciences Centre, Brighton and Sussex Medical School, Brighton, United Kingdom

## Synopsis

**We used the VERDICT framework to find clinically useful microstructural models to characterize vasculature in brain tumors. We correlated the vascular fractions, estimated by all possible three-compartment models, with perfusion MRI metrics (plasma volume and cerebral blood volume) derived from independent measurements on the same patients. The models with the strongest correlation with the perfusion MRI and clinical data incorporate spherical restriction for the intracellular compartment, isotropic diffusion for the extracellular compartment, and isotropically hindered or restricted pseudo-diffusion for the vascular compartment.**

## INTRODUCTION

Characterizing the microenvironment of brain tumors is crucial for diagnosis and therapy follow-up assessment, but current noninvasive imaging techniques fall short of this goal and clinicians often have to rely on invasive procedures, such as biopsy and histopathology<sup>1</sup>.

The cellular and vascular components of the tumor tissue are the most clinically relevant to characterize tumor biological attitude. Cellular composition can be assessed by diffusion-weighted MRI (dMRI): in areas of high cellularity, diffusion is strongly hindered or restricted. On the other hand, the vascular component is usually studied with perfusion MRI techniques such as dynamic contrast enhanced (DCE) or dynamic susceptibility contrast (DSC) MRI, which require contrast agent injection<sup>2,3</sup>. Alternatively, perfusion can also be detected by dMRI as areas of very high diffusivity (pseudo-diffusion)<sup>4</sup>.

VERDICT (Vascular, Extracellular, and Restricted Diffusion for Cytometry in Tumors) is a framework for multi-compartment modeling the vascular, extracellular and restricted component of tumor tissues<sup>5</sup>. It has shown diagnostic utility and high repeatability in body tumors, especially prostate cancer<sup>6,7</sup>. The aim of this study is to use the VERDICT framework to find a clinically useful microstructural model for brain tumors. In particular, we focus on the vascular component, and correlate our results (derived from dMRI) with independent perfusion MRI metrics such as the DCE-derived plasma volume (Vp), and the DSC-derived cerebral blood volume (CBV).

## METHODS

Data were collected from 5 patients (4 males, age 23-70); 3 had IDH wild-type anaplastic astrocytoma, one had a melanoma metastasis and one an IDH wild-type astrocytoma.

MRI was acquired at 3T (Ingenia CX, Philips Healthcare). A series of dMRI scans were acquired according to the scheme in Table 1. Four of the patients also had perfusion MRI including dynamic contrast enhanced (DCE) 3D spoiled gradient echo sequences (TE/TR=1.8/3.9 ms, flip angle 15°) and dynamic susceptibility contrast (DSC) fast field echo EPI sequences (TE/TR=31/1500 ms, flip angle 75°). Additionally, 3D-FLAIR images and post-contrast 3D T1-weighted images were acquired. Regions of interest (ROI) masks for the whole tumor were segmented on 3D-FLAIR images and for the tumor core on post-contrast 3D-T1 images, in order to outline the core and the periphery of the tumors (Figure 1).

After denoising, removal of Gibbs artifacts, motion and distortion correction, we fit multiple three-compartment models to the data in Matlab (MathWorks). Using the terminology in previous works<sup>8</sup>, a sphere was always used for intracellular restriction, whereas combinations of ball, zeppelin, tensor, stick, astrosticks and Watson-distributed sticks were used for the extracellular and vascular compartments, constraining the diffusivity to be at least  $3 \cdot 10^{-9} \text{ m}^2/\text{s}$  in the latter case. The name of each model is formed by the vascular compartment first, then the extracellular compartment, and finally the restricted compartment. As a reference we also fitted BallBallBall, which is equivalent to the triexponential extension of IVIM<sup>9</sup>.

Perfusion MRI data were analyzed with Olea Medical software (v 3.0, Olea Medical Solutions) to obtain parametric maps of Vp and CBV. The correlations between the derived metrics and the vascular fraction estimated by each model were evaluated with the Pearson coefficient.

## RESULTS

Figure 2 shows an example of the restricted and vascular fraction maps, with both fractions higher in the contrast-enhancing tumor core than in the periphery as expected.

Indeed, most of the models detected higher restriction in the tumor core than in the peritumoral areas, except for BallAstrosticksSphere and BallWatsonsticksSphere (not shown). BallBallBall, BallBallSphere and AstrosticksBallSphere detected higher vascular fractions in the contrast-enhancing core than in the peritumoral zone, but BallZeppelinSphere, BallTensorSphere and BallAstrosticksSphere actually estimated higher vascular fractions in the periphery (Figure 3).

The vascular fraction from AstrosticksBallSphere had the highest correlation with Vp:  $r=0.74$ , followed by BallBallBall ( $r=0.72$ ) and BallBallSphere ( $r=0.71$ ). The correlations with CBV were  $r=0.74$  for BallBallBall,  $r=0.68$  for AstrosticksBallSphere and  $0.64$  for BallBallSphere (Figure 4).

## DISCUSSION and CONCLUSION

We have tested multiple three-compartment models for the characterization of brain tumor microenvironments. Our preliminary results show that BallBallSphere and the more complex AstrosticksBallSphere could be able to characterize both restriction and vascularity of the tumors. As expected, they provided higher intracellular and vascular fractions in the core of the tumor than in the peritumoral area.

There was a certain degree of variability among patients, which could reflect the diverse biological features of the different lesions. In particular the highest values for both fractions are found in the melanoma metastasis of patient 4. The typical histopathological characteristics of this lesion include neoangiogenesis and densely-packed cells with high mitotic activity, possibly reflected by our models.

BallZeppelinSphere, BallTensorSphere and BallAstrosticksSphere estimated unrealistically high vascular fractions in the periphery areas, which likely correspond to areas of very high diffusivity which could not be properly modelled in the extracellular compartment by Zeppelin, Tensor or Astrosticks respectively. Similarly, BallAstrosticksSphere and BallWatsonsticksSphere estimated unrealistically high intracellular fractions in the periphery areas. This suggests that a Ball compartment needs to be included for extracellular diffusion in brain tumors.

If these results can be confirmed in a larger patient cohort and with further histopathology validation, our proposed models could significantly improve the diagnosis and therapeutic management of brain tumors, by providing a tool for the simultaneous evaluation of cellularity and vascularity of the lesions without need for contrast injection.

## Acknowledgements

## References

1. Ellingson BM, Wen PY, van den Bent MJ, Cloughesy TF. Pros and cons of current brain tumor imaging. *Neuro Oncol* 2014;16(Suppl7):vii2-vii11
2. Villanueva-Meyer JE, Mabray MC, Cha S. Current Clinical Brain Tumor Imaging. *Neurosurgery* 2017;81(3):397-415
3. Svolos P, Kousi E, Kapsalaki E, et al. The role of diffusion and perfusion weighted imaging in the differential diagnosis of cerebral tumors: a review and future perspectives. *Cancer Imaging* 2014; 14(1): 20
4. Le Bihan D. What can we see with IVIM MRI? *Neuroimage* 2019;187:56-67
5. Panagiotaki E, Walker-Samuel S, Siow B, et al. Noninvasive quantification of solid tumor microstructure using VERDICT MRI. *Cancer Res* 2014;74(7):1902-12
6. Panagiotaki E, Chan RW, Dikaios N, et al. Microstructural characterization of normal and malignant human prostate tissue with vascular, extracellular, and restricted diffusion for cytometry in tumours magnetic resonance imaging. *Invest Radiol.* 2015;50(4):218-27
7. Johnston EW, Bonet-Carne E, Ferizi U, et al. VERDICT MRI for Prostate Cancer: Intracellular Volume Fraction versus Apparent Diffusion Coefficient. *Radiology.* 2019;291(2):391-397
8. Panagiotaki E, Schneider T, Siow B, et al. Compartment models of the diffusion MR signal in brain white matter: a taxonomy and comparison. *Neuroimage.* 2012;59(3):2241-54
9. Ueda Y, Takahashi S, Ohno N, et al. Triexponential function analysis of diffusion-weighted MRI for diagnosing prostate cancer. *J Magn Reson Imaging.* 2016;43(1):138-48

## Figures

b (mm <sup>2</sup> /s)	50	70	90	110	350	1000	1500	2500	3000	3500	711	3000
TE (ms)	45	53	43	43	54	78	118	88	103	123	78	78
δ (ms)	5	5	5	5	10	10	10	20	15	15	20	20
Δ (ms)	22	30	20	20	26	50	90	50	70	90	42	42
N dir	3	3	3	3	3	3	3	3	3	3	38	63

Table 1: Acquisition parameters for the dMRI protocol. Abbreviations: b = b-value (degree of diffusion weighting), TE = echo time, δ = diffusion gradient duration, Δ = diffusion gradient separation, N dir = number of diffusion gradient directions

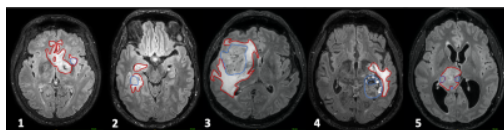


Figure 1: Representative 3D FLAIR images for each patient, with the tumor core and periphery outlined in blue and red respectively. Patient 1 was a 68-year-old female with an IDH wild-type anaplastic astrocytoma. Patient 2 was a 60-year-old male with an IDH wild-type anaplastic astrocytoma. Patient 3 was a 64-year-old male with an IDH wild-type anaplastic astrocytoma. Patient 4 was a 70-year-old male with a brain metastasis from melanoma. Patient 5 was a 23-year-old male with an IDH wild-type anaplastic astrocytoma.

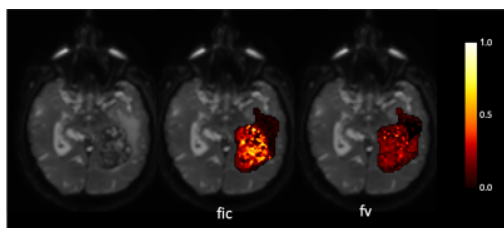


Figure 2: Representative maps of the intracellular fraction (fic) and vascular fraction (fv) derived by AstrosticksBallSphere in the tumor area of Patient 4, overlaid on the corresponding b = 0 image (also shown on the left for reference).



Figure 3: A) intracellular fraction ( $f_{ic}$ ) estimated by 6 representative models, averaged in the core (blue) and periphery (red) of each tumor. Note that BallBallBall doesn't model restriction in any of the three compartments; in this case  $f_{ic}$  is defined as the fraction of the compartment with lowest diffusivity. B) vascular fraction ( $f_v$ ) estimated by 6 representative models, averaged in the core (blue) and periphery (red) of each tumor.

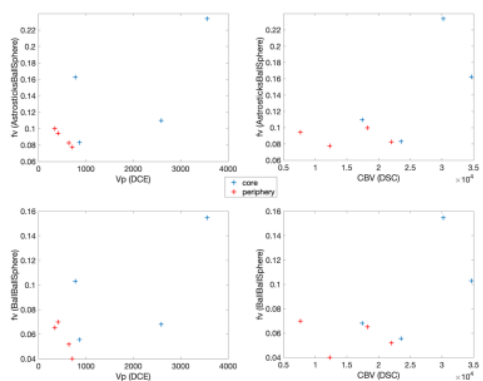


Figure 4: correlation between perfusion MRI and microstructure metrics. The average vascular fractions estimated by AstrosticksBallSphere (top) and BallBallSphere (bottom) in the core (blue) and periphery (red) of each lesion are plotted against the corresponding values of plasma volume (left) and cerebral blood volume (right).